Sliding Mode Control of a Spacecraft Power System

Mohammad Rasool Mojallizadeh and Bahram Karimi

Abstract: In this paper, the power electronic interface between a spacecraft electrical power system with a photovoltaic main source and battery storage as the secondary power source is modelled based on the state space averaging method. Subsequently, a novel sliding mode controller (SMC) is designed for maximum power point tracking (MPPT) of the PV array and load voltage regulation. Asymptotic stability is guaranteed through Lyapunov stability analysis. Afterwards, common Linear Quadratic Regulator (LQR), PID and Passivity-Based controllers (PBC)are provided to compare the results with those of the proposed sliding mode controller responses. Simulation of the hybrid system is accomplished using MATLAB and results are very promising.

Keywords: Sliding mode control, spacecraft EPS, PV/battery hybrid system, LQR, PID, PBC .

1. Introduction

The electrical power system (EPS) is the most critical system on any spacecraft. Power is used for communications, vehicle attitude control, guidance, propulsion, and in all equipments of the payload [1]. Spacecraft power subsystems typically comprise PV array, rechargeable batteries, and DC/DC converters. DC/DC converters are switched systems. It means that their operation is characterized by a switching of circuit topologies, which gives rise to a variety of nonlinear behavior. This nonlinear behavior is usually avoided by the engineers, who prefer to adjust system's parameters so that the system operates on a well-behaved region where the linear approximations are applicable, and so they can use classical methods of stability analysis and control [2].

Linear Quadratic Regulator (LQR), which is a very significant theory in Modern Control [3]. The LQR method has its advantages as standard design, easy realization and being able to gain linear feedback structure [4]. LQR can be straightforwardly calculated from the matrices of the small-signal state-space averaged model of the system[5].
Proportional Integral derivative (PID), which has dominated the practice for over 80 years [6]. The usefulness of PID controls lies in their general applicability to most control systems. In particular, when the mathematical model of the plant is not known and therefore analytical design methods cannot be used, PID controls prove to be most useful.

Manuscript received August 7, 2013; accepted October 13, 2013.
M. R. Mojallizadeh is with the Department of Electrical and Computer Engineering, Tabriz University, Iran.
B. Karimi is with the Department of Electrical Engineering, Malek Ashtar University of Technology, Shahinshahr, Isfahan, Iran.
The corresponding author's email is: bahram-karimi@aut.ac.ir

In the field of process control systems, it is well known that the basic and modified PID control schemes have proved their usefulness in providing satisfactory control, although in many given situations they may not provide optimal control [7]. Traditionally the PID controller is one of the mostly used to carry out control of the DC/DC converters[8].

Passivity-based control (PBC) was introduced by Ortega et al. as a controller design methodology that achieves stabilization by passivation. PBC methods are characterized by their robustness, a property that usually lacked in linear control methods such as PID and LQR. PBC also results in the simpler control laws[9].

Sliding mode control (SMC) is popular to converters [10]. The application of SMC to DC/DC converters can be traced back to 1983 [11]. The SMC design theory and application examples are available in [12]. SMC offers several benefits, namely, large signal stability, robustness, good dynamic response, system order reduction, and simple implementation [13]. A typical sliding mode control has two modes of operation. One is called the approaching mode, where the system state converges to a pre-defined manifold named sliding function in finite time. The other mode is called the sliding mode, where the system state is confined on the sliding surface and is driven to the origin [12]. SMC is compatible with a wide range of processors such as DSP, microcontroller, FPGA, etc.[14].

Tracking the maximum power point (MPP) of a photovoltaic (PV) array is usually an essential part of a PV system. As such, many MPP tracking (MPPT) methods have been developed and implemented. The methods vary in complexity, sensors required, convergence speed, cost, range of effectiveness, implementation hardware, popularity, and in other respects[15]. Common control approaches required reference current for control law synthesis and may lead to a lack of robustness to operation conditions[16]. This reference current comes from MPPT algorithms [17]. Moreover, the requirement for external MPPT algorithms may increase the weight, volume and complexity of the EPS. By deliberately defining the novel sliding surface a robust SMC approach was proposed in this paper.

This study presents SMC control of a Pv/battery hybrid system for MPPT of the PV array, load voltage regulating, and charging or discharging the battery. The basic idea is that the sliding surfaces are defined as the slope of P-I curve and battery current error. Asymptotic stability of the proposed system is guaranteed through Lyapunov stability analysis. Afterwards, common controllers are provided to compare the results with those of the proposed sliding mode controller responses.

The paper is organized as follows. System modeling is introduced in Section 2. In Section 3, design and analysis of the SMC are presented. Common LQR, PID and PBC controllers are provided in section 4 for comparison with the proposed control approach. Simulation results in MATLAB environment are then used in Section 5 to demonstrate the effectiveness of the proposed controllers. Finally, Section 6 concludes the paper.

2. System Modeling

The proposed spacecraft power system is depicted in Fig. 1. This power source comprises a PV array, a battery storage, DC/DC converters and load. The battery storage has been considered for conditions in which the load power exceeds the generating power of the PV array.

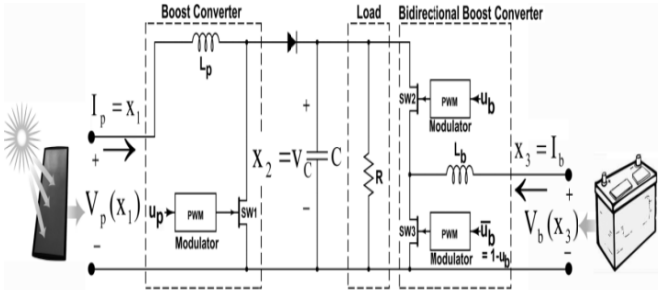

Fig. 1. Proposed system diagram.

2.1. Solar Energy System

A solar cell is the fundamental component of a PV system, which converts the solar energy into electrical energy. A solar cell consists of a p-n junction semiconductor material. A PV array consists of a certain number of solar cells connected in series to provide the desired voltage. The equivalent circuit of a solar cell is depicted in Fig. 2.

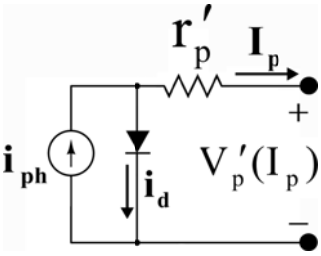

Fig. 2. Equivalent circuit of the solar cell.

The equivalent circuit mainly consists of a current source (i_{ph}), which amplitude depends on irradiance and temperature, diode, and internal resistance (r'_p). The P-I characteristic of a solar cell is highly nonlinear and is given by the following equations [18]:

$$V'_p = \left(k_b TA/q\right)\ln\left(\left(i_{ph}+i_0-I_p\right)/i_0\right)-I_p r'_p,\ V_p = nV'_p \quad (1)$$

$$i_{ph} = \lambda\left[i_{sc} + k_i\left(T - T_r\right)\right] \quad (2)$$

$$i_0 = i_r\left[T/T_r\right]^3 \exp\left(\left(qE_g/\left(k_b A\right)\right)\left(1/T_r - 1/T\right)\right) \quad (3)$$

where V'_p is the solar cell voltage, Vp is the PV array voltage, Ip is the solar cell and PV array current, n is the number of series cells, i_0 is the diode reverse saturation current, q is the electron charge, A is the ideality factor of the p-n junction, k_b is the Boltzmann constant, k_i is the temperature coefficient, T is the cell temperature, T_r is the reference temperature, E_g is the band-gap energy in eV, i_r is the saturation current at T_r, and i_{sc} is the short circuit current.

Fig. 3 shows the P-I curve of the SM-55 PV array under different irradiance conditions. The power delivered by the PV module depends on the solar irradiance and cell temperature. Thus, maximum power must be available under different conditions.

The PV array efficiency can be calculated as the ratio of solar power in experiment ($V_p I_p$) to maximum theoretical power.

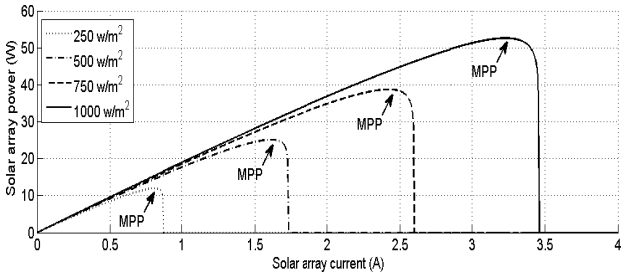

Fig. 3. PV array characteristic under different irradiance levels.

2.2. Battery Storage

Storage devices are utilized for energy storage in hybrid power sources. The batteries store energy in the electrochemical form. In this study, the battery is modelled based on the genericTheveninmodel [19]. Fig. 4 shows equivalent circuit of the battery.

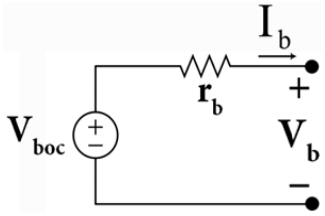

Fig. 4. Equivalent circuit of the Battery storage.

Battery voltage and State of Charge (SoC) can be calculated by Eq. (4):

$$V_b = V_{boc} - r_b I_b$$
$$E(t) = -\int \left(\beta V_{boc} I_b + W_{Loss}\right) dt, \quad \beta = \begin{cases} \beta_1 & I_b > 0 \\ \beta_2 & I_b < 0 \end{cases} \qquad (4)$$
$$SoC(t) = E(t) / E_{Max}$$

where V_{boc} is the open circuit voltage, r_b is the equivalent resistance, β_1 is discharging constant, β_2 is the charging constant, W_{Loss} is battery loss, $E(t)$ is battery energy and E_{Max} is maximum battery energy.

2.3. DC/DC Converters

The amplitude of the DC output current (voltage) of the PV system depends on the solar irradiance delivered to the PV arrays. Therefore, a boost DC/DC converter is utilized to adjust the output current of the PV system. Also, a bidirectional DC/DC converter is used for load voltage regulation and chargesor discharges the battery storage. The DC/DC converters have been depicted in Fig. 1.

From Fig. 5 the system can be written in four sets of state equation depends on the position of switches SW1, SW2, and SW3. By utilizing state space averaging method [20], dynamic equations of the system can be expressed as Eq. (5):

$$\begin{cases} \dot{x}_1 = \left(V_p(x_1) - x_2 + x_2 u_p\right) / L_p \\ \dot{x}_2 = \left(-\frac{1}{R} x_2 + x_1 - x_1 u_p + x_3 u_b\right) / C \\ \dot{x}_3 = \left(V_b - x_2 u_b\right) / L_b \end{cases} \qquad (5)$$

where, $\mathbf{x} = [x_1, x_2, x_3]^T = [i_{L_p}, v_C, i_{L_b}]^T$ is the state vector, $0 < u_p < 1$ is the duty cycle of SW1 which is also a control input for MPPT, and $0 < u_b < 1$ is the duty cycle of SW2 which is also a control input for regulating load voltage and charging or discharging battery. Eq. (5) can be written in general form of the nonlinear time invariant system:

$$\dot{\mathbf{x}} = f(\mathbf{x}) + g(\mathbf{x})\mathrm{u} \qquad (6)$$

3. Sliding mode controller design

In the proposed stand-alone hybrid system, the main objectives are MPPT tracking of the PV array and load voltage regulation. In this study, a novel MIMO sliding mode controller designed for these purposes. The proposed controller produces two control signals. The first control

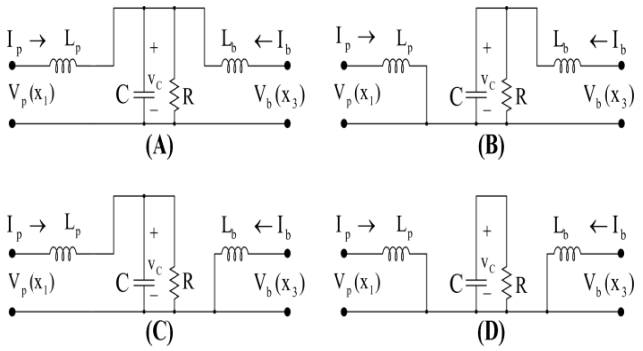

Fig. 5. Different operating conditions. (A): SW1=O, SW2=C, SW3=O. (B): SW1=C, SW2=C, SW3=O. (C): SW1=O, SW2=O, SW3=C. (D): SW1=C, SW2=O, SW3=C. (Open=O and Close=C).

signal (u_p), applied to the boost converter for the MPPT of the PV array and the second control signal (u_b) applied to the bidirectional boost converter for load voltage regulation. Fig. 3 shows P-I curve of the PV array under uniform insolation conditions. By selecting the PV sliding surface as (7) it is guaranteed that the system state will hit the surface and produce maximum power persistently.

$$\partial P_P / \partial I_P = \partial\left(I_P^2 R_P\right) / \partial I_P = I_P\left(2R_P + I_P \partial R_P / \partial I_P\right) = 0 \qquad (7)$$

where, $R_p = V_p / I_p$ is the equivalent impedance. The non-trivial solution of (7) selected as PV sliding surface (s_p):

$$s_p \triangleq 2R_P + I_P \partial R_P / \partial I_P \qquad (8)$$

With $R_p = V_p / I_p$ Eq. (8) can also be written as Eq.(9):

$$s_p \triangleq 2V_p(x_1)/x_1 + x_1 \partial\left(V_p(x_1)/x_1\right) / \partial x_1 \qquad (9)$$

voltage regulation sliding surface (s_b) also selected as Eq. (10):

$$s_b = x_3 - x_{3d} \qquad (10)$$

where, x_{3d} is the desired battery current and can be described by Eq. (11):

$$P_b = P_L - P_p \rightarrow x_{3d} = \frac{1}{V_b}\left(\frac{1}{R} x_{2d}^2 - V_p x_1\right) \qquad (11)$$

here, P_b, P_L, and P_p are battery power, load power, and PV power respectively. By considering the sliding surface vector as Eq. (12) it is guaranteed that the system will reach its desired states:

$$\mathbf{s}=\begin{bmatrix} s_p \\ s_b \end{bmatrix}=\begin{bmatrix} 2v_p(x_1)/x_1+x_1\,\partial\left(v_p(x_1)/x_1\right)/\partial x_1 \\ x_3-x_{3d} \end{bmatrix} \quad (12)$$

where, $\partial\left(v_p(x_1)/x_1\right)/\partial x_1$ can be obtained by using

$$\frac{\partial\left(V_p(x_1)/x_1\right)}{\partial x_1}=\frac{V_p(x_1(\mathrm{k}))/x_1(\mathrm{k})-V_p(x_1(\mathrm{k}-1))/x_1(\mathrm{k}-1)}{x_1(\mathrm{k})-x_1(\mathrm{k}-1)}$$

In order to get the equivalent control ($\mathbf{u}_{eq}$) suggested by [12], the equivalent control is determined from the following condition.

$$\dot{\mathbf{s}}=\begin{bmatrix} \frac{\partial s_p}{\partial x_1}\dot{x}_1+\frac{\partial s_p}{\partial x_2}\dot{x}_2+\frac{\partial s_p}{\partial x_3}\dot{x}_3 \\ \frac{\partial s_b}{\partial x_1}\dot{x}_1+\frac{\partial s_b}{\partial x_2}\dot{x}_2+\frac{\partial s_b}{\partial x_3}\dot{x}_3 \end{bmatrix}_{\mathbf{u}=\mathbf{u}_{eq}}=\begin{bmatrix} \frac{\partial s_p}{\partial x_1}\dot{x}_1 \\ \frac{\partial s_b}{\partial x_3}\dot{x}_3 \end{bmatrix}_{\mathbf{u}=\mathbf{u}_{eq}}=\begin{bmatrix} 0 \\ 0 \end{bmatrix} \quad (13)$$

The equivalent control is then derived.

$$\mathbf{u}_{eq}=\begin{bmatrix} u_{peq} \\ u_{beq} \end{bmatrix}=\begin{bmatrix} 1-\frac{V_p(x_1)}{x_2} \\ \frac{V_b}{x_2} \end{bmatrix} \quad (14)$$

Since the range of duty cycle must lies in $0<\left(u_p,u_b\right)<1$, the real control signal is proposed as:

$$\mathbf{u}=\begin{bmatrix} u_p \\ u_b \end{bmatrix} \quad (15)$$

where, u_p and u_b can be written as:

$$u_p=\begin{cases} 0 & u_{peq}+k_p s_p<0 \\ u_{peq}+k_p s_p & 0<u_{peq}+k_p s_p<1 \\ 1 & 1<u_{peq}+k_p s_p \end{cases} \quad (16)$$

$$u_b=\begin{cases} 0 & u_{beq}+k_b Sat(s_b/\phi)<0 \\ u_{beq}+k_b Sat(s_b/\phi) & 0<u_{beq}+k_b Sat(s_b/\phi)<1 \\ 1 & 1<u_{beq}+k_b Sat(s_b/\phi) \end{cases} \quad (17)$$

where k_p and k_b are constant coefficients and are determined by trial and error method by using computer simulations, $Sat(s)$ is the saturation function which is shown in Fig. 6, and ϕ is a small constant and is selected for chattering avoidance [12].

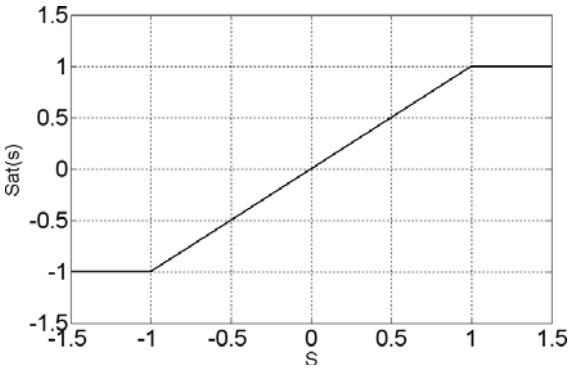

Fig. 6. Saturation function.

The existence of the approaching mode of the proposed sliding function s is provided. A Lyapunov function is defined as:

$$v=v_M+v_R \quad (18)$$

where, v_M and v_R are positive definite terms and defined as:

$$v_M=\frac{1}{2}s_p^2 \quad , \quad v_R=\frac{1}{2}s_b^2 \quad (19)$$

The time derivative of v can be written as:

$$\dot{v}=\dot{v}_M+\dot{v}_R \quad (20)$$

The achievability of $s=0$, will be obtained by $\dot{v}<0$. It can be shown that both $\dot{v}_M$ and $\dot{v}_R$ are negative definite. $\dot{v}_R$ can be written as follow:

$$\dot{v}_R=s_b\left(V_b-x_2u_b\right)/L_b \quad (21)$$

Three cases should be examined for the fulfillment of $\dot{v}_R<0$:

FOR $0<u_b<1$

$$\dot{v}_R=-x_2k_b\left(x_3-x_{3d}\right)sat\left(\frac{x_3-x_{3d}}{\phi}\right)/L_b<0 \quad (22)$$

Since, $\left(x_3-x_{3d}\right)$ always has same sign of $sat\left(\frac{x_3-x_{3d}}{\phi}\right)$ and $x_2k_b>0$, the sign of (22) is negative definite.

FOR $u_b=1$

$$\dot{v}_R=s_b\left(V_b-x_2\right)/L_b<0 \quad (23)$$

In this case, the load voltage (x_2) is higher than the battery voltage (V_b)and $s_b > 0$. from (23) it results $\dot{v}_R < 0$.

FOR $u_b = 0$

$$\dot{v}_R = s_b V_b / L_b < 0 \quad (24)$$

In this case, $s_b < 0$ is obtained and $\dot{v}_R < 0$. From the discussion above $\dot{v}_R < 0$ is obtained.

$\dot{v}_M$ can also be written as:

$$\dot{v}_M = (s_p \dot{s}_p) \quad (25)$$

The time derivative of s_p can be written as:

$$\dot{s}_p = \left(3\partial R_p / \partial x_1 + x_1 \partial^2 R_p / \partial x_1^2\right)\left(V_p(x_1) - x_2 + x_2 u_p\right) / L_p \quad (26)$$

Replacing R_p by the definition of $R_p = V_p / I_p$:

$$\frac{\partial R_p}{\partial x_1} = \frac{\partial}{\partial x_1}\left[\frac{V_p}{x_1}\right] = \frac{1}{x_1}\frac{\partial V_p}{\partial x_1} - \frac{V_p}{x_1^2} \quad (27)$$

$$\frac{\partial^2 R_p}{\partial x_1^2} = \frac{1}{x_1}\frac{\partial^2 V_p}{\partial x_1^2} - \frac{2}{x_1^2}\frac{\partial V_p}{\partial x_1} + \frac{2V_p}{x_1^3} \quad (28)$$

By (1), the following equations will be obtained:

$$\frac{\partial V_p(x_1)}{\partial x_1} = -n\frac{k_b T A}{q}\frac{i_0}{i_{ph} + i_0 - x_1} - r_p < 0 \quad (29)$$

$$\frac{\partial^2 V_p(x_1)}{\partial x_1^2} = -n\frac{k_b T A}{q}\frac{i_0}{\left(i_{ph} + i_0 - x_1\right)^2} < 0 \quad (30)$$

Substitute (29) and (30) into $\partial s_p / \partial x_1$ yield:

$$\frac{\partial s_p}{\partial x_1} = 3\frac{\partial R_p}{\partial I_p} + I_p \frac{\partial^2 R_p}{\partial I_p^2} = \frac{\left(\partial v_p(x_1)/\partial x_1\right)}{x_1} + \frac{\partial^2 V_p(x_1)}{\partial x_1^2} - \frac{V_p}{x_1^2} < 0 \quad (31)$$

According to the result of (29), (30) and $\left(V_p, x_1\right) > 0$, the sign of (31) is negative definite. The achievability of $\dot{v}_M < 0$ will be obtained by $s_p \dot{s}_p < 0$ for all u_p discussed as follows.

FOR $0 < u_p < 1$

$$\dot{x}_1 = \left(V_p(x_1) - x_2\left(1 - u_{peq} - k_p s_p\right)\right) / L_P = x_2 k_p s_p / L_p \quad (32)$$

Based on the result of (31) and (32) $\dot{s}_p$ always has inverse sign of s_p . Therefore, $s_p \dot{s}_p < 0$ is obtained for $0 < u_p < 1$.

FOR $u_p = 1$

$$\dot{x}_1 = V_p(x_1) / L_p > 0 \quad (33)$$

By (31) and (32), $\dot{s}_p < 0$. with $u_p = 1$, two cases should be examined for the fulfillment of $s_p \dot{s}_p < 0$.

A) $u_{peq} = 1$

If $u_{peq} = 1$, it implies $V_p(x_1) = 0$ which means s_p is negative for this case. Therefore, $u_{peq} + k_p s_p$ will be less than 1, which contradicts to the assumption of $u_p = 1$.

B) $u_{peq} < 1$ and $u_{peq} + k_p s_p \geq 1$

If $u_{peq} < 1$, and $u_{peq} + k_p s_p \geq 1$, it implies $s_p > 0$ and $s_p \dot{s}_p < 0$.

It conclude that $s_p \dot{s}_p < 0$ for $u_p = 1$.

FOR $u_p = 0$

$$\dot{x}_1 = \left(V_p(x_1) - x_2\right) / L_p \quad (34)$$

In this case load voltage is higher than the PV voltage ($V_p(x_1) < x_2$). From (31) and (33), it results that $\dot{s}_p > 0$. Two cases for $u_p = 0$ are examined as follows.

A) $u_{peq} = 0$

$u_{peq} = 0$ implies $V_p(x_1) = x_2$, which contradicts to the assumption of $V_p(x_1) < x_2$.

B) $u_{peq} > 0$ and $u_{peq} + k_p s_p \leq 0$

In this case, $s_p < 0$ is obtained and $s_p \dot{s}_p < 0$.

It concludes that $s_p \dot{s}_p < 0$ for $u_p = 0$. From the discussion above, the stability of the system can be guaranteed using the proposed control law (16) and (17).

4. Common Control Methods

In this study common LQR, PID and PBC approaches [16] provided to compare the results with those of the proposed sliding mode controller responses. Note that common control methods required reference current (x_{1d}) for control law synthesis and may lead to a lack of robustness to operation conditions. In the following equations, x_{3d} is

the desired battery current and can be described by Eq. (11) and x_{2d} is the reference of the load voltage.

4.1. Linear Quadratic Regulator

The design of a LQR controller is based on the average model of converters. Then, the linearized model of the converter around an equilibrium point and MATLAB functions are used to design LQR controller (see [21] for more details). The linearized model of the system can be written as Eq. (35):

$$\begin{bmatrix} \dot{x}_1 \\ \dot{x}_2 \\ \dot{x}_3 \end{bmatrix} = \mathrm{A} \begin{bmatrix} x_1 \\ x_2 \\ x_3 \end{bmatrix} + B \begin{bmatrix} u_p \\ u_b \end{bmatrix}$$
$$\begin{bmatrix} y_1 \\ y_2 \end{bmatrix} = C \begin{bmatrix} x_1 \\ x_2 \\ x_3 \end{bmatrix} + D \begin{bmatrix} u_p \\ u_b \end{bmatrix} \quad (35)$$

Since the MATLAB LQR function is unable to solve the regulation problems, the following equations are used to convert regulation problem into stabilization problem [21].

$$\begin{aligned} z_{11} &\triangleq x_1 - 2x_{1d} \\ z_{12} &\triangleq x_2 - 2x_{2d} \\ z_{13} &\triangleq x_3 - 2x_{3d} \\ u'_p &\triangleq u_p - 2u_p^{ss} \\ u'_b &\triangleq u_b - 2u_b^{ss} \\ z_{21} &\triangleq g_1 = \int_0^t (x_1 - 2x_{1d})\, dt \\ z_{22} &\triangleq g_2 = \int_0^t (x_2 - 2x_{3d})\, dt \end{aligned} \quad (36)$$

By applying Eq.(36), Eq.(35) can be written as:

$$\begin{bmatrix} \dot{z}_{11} \\ \dot{z}_{12} \\ \dot{z}_{13} \\ \dot{z}_{21} \\ \dot{z}_{22} \end{bmatrix} = A' \begin{bmatrix} z_{11} \\ z_{12} \\ z_{13} \\ z_{21} \\ z_{22} \end{bmatrix} + B' \begin{bmatrix} u'_p \\ u'_b \end{bmatrix} \quad (37)$$
$$A' = \begin{bmatrix} A_{3\times3} & \mathbf{0}_{3\times2} \\ C_{2\times3} & \mathbf{0}_{2\times2} \end{bmatrix} \quad , \quad B' = \begin{bmatrix} B \\ D \end{bmatrix}$$

The feedback gain can be calculated by the following MATLAB command:

$$>> \; K = lqr(\mathrm{A}', \mathrm{B}', \mathrm{Q}, \mathrm{R}) \quad (38)$$

where R and Q are determined by trial and error method by using computer simulations. Finally, the LQR control can be written as:

$$\begin{bmatrix} u_p \\ u_b \end{bmatrix} = -K \begin{bmatrix} x_1 - x_{1d} & x_2 - x_{2d} & x_3 - x_{3d} & g_1 & g_2 \end{bmatrix}^T \quad (39)$$

4.2. Proportional Integral Derivative

PID control law can be calculated by Eq. (40):

$$\begin{aligned} u_p &= sat\left(k_{p1}\, e_p + k_{p2}\, \dot{e}_p + k_{p3} \int_0^t e_p\, dt\right) \\ u_b &= sat\left(k_{b1}\, e_b + k_{b2}\, \dot{e}_b + k_{b3} \int_0^t e_b\, dt\right) \\ e_p &= x_1 - x_{1d} \quad , \quad e_b = x_3 - x_{3d} \end{aligned} \quad (40)$$

where k_{p1}, k_{p2}, k_{p3}, k_{b1}, k_{b2} and k_{b3} are determined by trial and error method [22].

4.3. Passivity Based Control

The design of the PBC controller is based on the Euler Lagrange model of the converters. The PBC control signals which proposed in [16] are shown in Eq. (41) and (42).

$$u_p = 1 - \frac{1}{x_{2d}} \left(V_p(x_1) + r_{a1}\left(x_1 - x_{1d}\right)\right) \quad (41)$$

$$u_b = \frac{1}{x_{2d}} \left(V_b(x_3) + r_{a2}\left(x_3 - x_{3d}\right)\right) \quad (42)$$

$\left(r_{a1}, r_{a2}\right) > 0$ are design parameters (see [16] for more details).

5. Simulation

MATLAB environment is used to investigate the performance of the novel SMC on a Spacecraft EPS.LQR, PID and PBCcontrollers are provided to compare the results with those ofthe proposedSMC responses. The simulation investigatesfour system characteristics: robustness against irradiance, temperature, load resistance,and load voltage reference changes. Unlike SMC,common approaches required reference current (x_{1d}) for control law synthesis which comes from P&O algorithm[16]. It is assumed that optimal reference current (x_{1d}) is available to common LQR, PID and PBC controllers.The parameters of the components are chosen to deliver maximum 55 W of power generated by SM-55 and battery.Simulation conditions with fourstep changes are shown in Table 1:

Table 1. Parameters variations.

Load (Ω)	**Temperature (℃)**	**Irradiance (W/m^2)**	**Time (s)**
70	10	400	0-2
70	10	1000	2-4
70	50	1000	4-6

30	50	1000	6-8

In order to compare the proposed control method with other approaches, four performance functions have been defined as follow:

1) Efficiency function (J_{Eff}): This function is defined as Eq. (43). Lower J_{Eff} indicates higher PV array efficiency.

$$J_{Eff} = \int_0^t \left(x_1 - x_{1d}\right)^2 dt \tag{43}$$

2) Conditioning function (J_{Reg}): This function is defined as Eq. (44). Lower J_{Reg} indicates better voltage regulation.

$$J_{\mathrm{Reg}} = \int_0^t \left(x_2 - x_{2d}\right)^2 dt \tag{44}$$

3) Battery saving function: This function is defined as Eq. (45). Higher ΔSoC indicates grater battery saving.

$$\Delta SoC = SoC(t_f) - SoC(t_0) \tag{45}$$

where $SoC(t_0)$ is the initial SoC and $SoC(t_f)$ is the final SoC.

$42.5^{(V)}$ sun-regulated busses have been used on many small satellites [23], Therefore, load voltage reference (x_{2d}) is selected as $42.5^{(v)}$.

Fig. 7 shows PV array current. LQR controllershows long settling time and therefore lower transient efficiency. PID controller exhibits steady tracking error and therefore lower steady efficiency. Unlike the proposed controller, PBC and other common methods required reference current for control law synthesis and may lead to a lack of robustness. The comparison of PV array current based on SMC and other controllers demonstrates that the proposed controller exhibits a smooth and fast transient. According to Table 2 theproposed system has lower J_{Eff} and thereforehas higher efficiency.

Fig. 8 shows load voltage. LQR controller exhibits overshoot which may damages the load. PID controller shows steady state error which is not desired. Unlike Linear methods, PBC and the proposed controller track the voltage reference well. According toTable 2. the proposed system has lower J_{Reg} and therefore has better tracking performance.

Fig. 9 shows PV array efficiency. The proposed controller has sufficient efficiency.

Fig. 10 demonstrates battery state of charge. The initial SoC is equal to 50%. According to Table 2. the proposed system has higher ΔSoC and therefore has better battery saving.

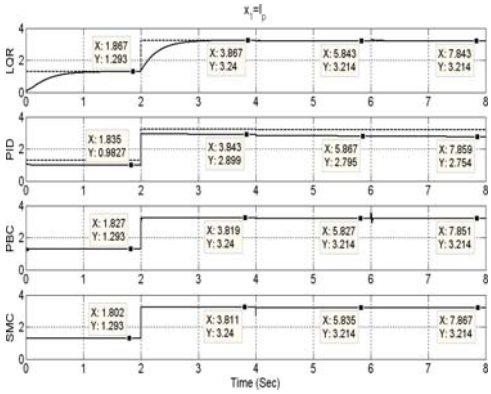

Fig. 7. PV array current.

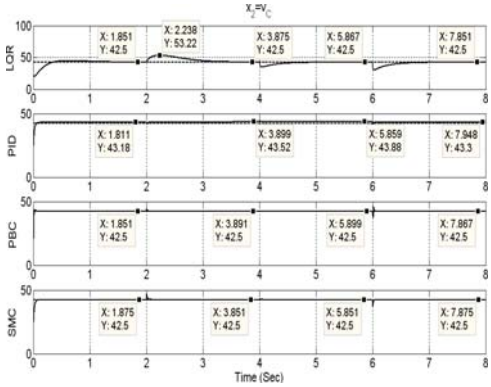

Fig. 8. Load voltage.

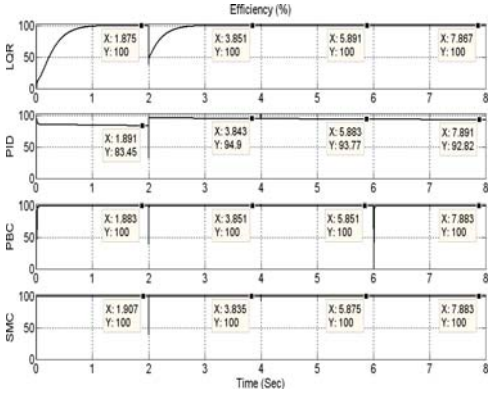

Fig. 9. PV array efficiency.

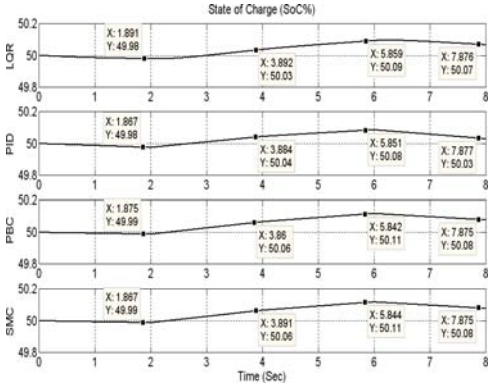

Fig.10. Battery State of Charge (SoC).

Fig.11 and Fig. 12 show control signals. Due to use of the saturation function in the proposed control signal, the proposed sliding mode controller has no chattering problem of traditional variable structure sliding mode controller [12].

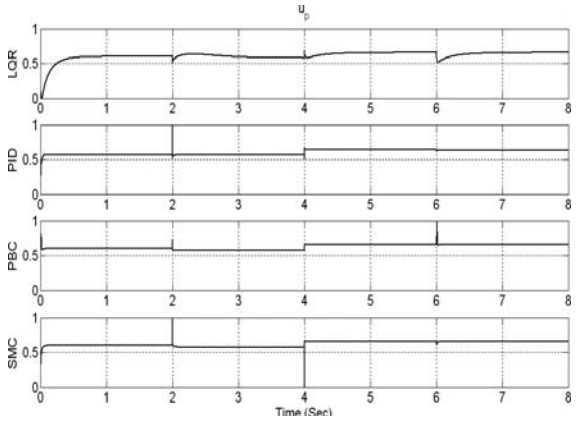

Fig.11. u_p control signal.

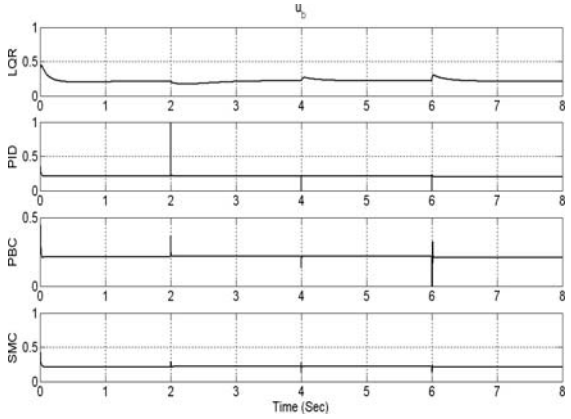

Fig.12. u_b control signal.

Table 2. Performance of each control method.

ΔSoC%	J_{Reg}	J_{Eff}	Control Method
+0.0680	148.9197	0.8259	LQR
+0.0300	15.2294	1.1029	PID
+0.0771	11.2499	0.0059	PBC
+0.0782	9.3327	0.0030	The proposed SMC

6. Results

In this paper, a state space averaging model of a stand-alone hybrid dc power source with a PV array as the main source, a battery storage as the secondary source and interfacing DC/DC converters which is used as the spacecraft EPS has been presented.Subsequently, sliding mode controller has been designed to control the interfacing DC/DC converters. Asymptotic stability of the proposed system is guaranteed through Lyapunov stability analysis

To investigate the validity of the proposed system, common LQR, PID and PBC controllers were provided. Simulation results showLQR controller has high overshoot and long settling time. PID controller exhibits steady state error. Unlike the proposed SMC, PBC controller and other Common approaches required reference current for control law synthesis and may lead to a lack of robustness to operation conditions.

The results of the proposed control system haslow overshoot, short settling time and zero steady-state errorcompared to those of the linear controller results. In other words, the proposed system has higher efficiency, better voltage regulating and better battery saving. Moreover, the aforementioned results demonstrate the robustness of the proposed control approach during the load resistance, battery voltage, solar irradiance, PV array temperature,andload voltage reference changes.

Table 3. Nomenclature.

Value	Parameter
$5(mH)$	L_p
$10(mH)$	L_b
$500(\mu f)$	C
$30(m\Omega)$	r_p
36	n
$55(w)$	Maximum PV array power
$3.45(A)$	PV array short circuit current
$21.7(v)$	PV array open circuit voltage
$25℃$	T_r
$1.2(A/k)$	k_i
$5.98\times10^{-8}(A)$	i_r
$1.12(ev)$	E_g
1.2	A
$9(v)$	V_{boc}
0.9	β_1
1.1	β_2
$20(wh)$	Battery Capacity
$10(mw)$	W_{Loss}
$80(m\Omega)$	r_b
$1.381\times10^{-23}(J/K)$	k_b
$1.6\times10^{-19}(C)$	q

References

[1] L. F. R. Turci, E. E. N. Macau, and T. Yoneyama, "Efficient chaotic based satellite power supply subsystem," *Chaos, Solitons and Fractals*, vol. 42, pp. 396-407, 2009.

[2] Q. He, L. Long, and J. Zhao, "Comparative analysis of three nonlinear controllers for boost converters and switching design," in *31st Chinese Control Conference*, Hefei, China, pp. 870-875, 2012.

[3] C. Olalla, R. Leyva, A. El Aroudi, and I. Queinnec, "Robust LQR Control for PWM Converters: An LMI Approach," *IEEE Transactions on Industrial Electronics*, vol. 56, pp. 2548-2558, 2009.

[4] F. H. Dupont, V. F. Montagner, J. R. Pinheiro, H. Pinheiro, S. V. G. Oliveira, and A. Peres, "Comparison of digital LQR techniques for DC-DC boost converters with large load range," in *2011 IEEE International Symposium on Circuits and Systems (ISCAS)*, Rio de Janeiro, Brazil, pp. 925-928, 2011.

[5] C. Jaen, J. Pou, R. Pindado, V. Sala, and J. Zaragoza, "A Linear-Quadratic Regulator with Integral Action Applied to PWM DC-DC Converters," in *IEEE Industrial Electronics, IECON 2006* - 32nd Annual Conference on, pp. 2280-2285, 2006.

[6] A. Kiam Heong, G. Chong, and L. Yun, "PID control system analysis, design, and technology," *IEEE Transactions on Control Systems Technology*, vol. 13, pp. 559-576, 2005.

[7] V. Duchaine, S. Bouchard, and C. M. Gosselin, "Computationally efficient predictive robot control," *IEEE/ASME Transactions on Mechatronics*, vol. 12, pp. 570-578, 2007.

[8] M. D. Pedroso, C. B. Nascimento, A. M. Tusset, and M. D. S. Kaster, "Performance comparison between nonlinear and linear controllers applied to a buck converter using poles placement design," in *15th European Conference on Power Electronics and Applications (EPE)*, 2013, pp. 1-10, 2013.

[9] R. Ortega, A. van der Schaft, B. Maschke, and G. Escobar, "Interconnection and damping assignment passivity-based control of port-controlled Hamiltonian systems," *Automatica*, vol. 38, pp. 585-596, Apr. 2002.

[10] V. Utkin, "Sliding mode control of DC/DC converters," *Journal of the Franklin Institute*, vol. 350, pp. 2146-2165, Oct. 2013.

11] F. Bilalovic, O. Music, and A. Sabanovic, "Buck converter regulator operating in the sliding mode," in *7th Power Conversion International Conf.*, pp. 331–340, 1983.

[12] J. J. E. Slotine and W. Li, *Applied Nonlinear Control*. United States: Addison Wesley, 2005.

[13] P. Mattavelli, L. Rossetto, and G. Spiazzi, "Small-signal analysis of DC-DC converters with sliding mode control," *IEEE Transactions on Power Electronics*, vol. 12, pp. 96-102, 1997.

[14] B. Subudhi and R. Pradhan, "A comparative study on maximum power point tracking techniques for photovoltaic power systems," *IEEE Transactions on Sustainable Energy*, vol. 4, pp. 89-98, 2013.

[15] T. Esram and P. L. Chapman, "Comparison of photovoltaic array maximum power point tracking techniques," *IEEE Transactions on Energy Conversion*, vol. 22, pp. 439-449, 2007.

[16] A. Tofighi and M. Kalantar, "Power management of Pv/battery hybrid power source via passivity-based control," *Renewable Energy*, vol. 36, pp. 2440-2450, Sept. 2011.

[17] M. A. G. de Brito, L. Galotto, L. P. Sampaio, G. de Azevedo e Melo, and C. A. Canesin, "Evaluation of the main MPPT techniques for photovoltaic applications," *IEEE Transactions on Industrial Electronics*, vol. 60, pp. 1156-1167, 2013.

[18] H. El Fadil and F. Giri, "Climatic sensorless maximum power point tracking in PV generation systems," *Control Engineering Practice*, vol. 19, pp. 513-521, May 2011.

[19] B. Lin, "Conceptual design and modeling of a fuel cell scooter for urban asia," M.Sc. Thesis, Mechanical and Aerospace Engineering, Princeton University, Princeton, New Jersey, United States, 1999.

[20] P. T. Krein, J. Bentsman, R. M. Bass, and B. L. Lesieutre, "On the use of averaging for the analysis of power electronic systems," *IEEE Transactions on Power Electronics*, vol. 5, pp. 182-190, 1990.

[21] F. L. Lewis, D. L. Vrabie, and V. L. Syrmos, *Optimal Control*, Third ed., New Jersey, United States: Wiley, 2012.

[22] S. W. Sung, J. Lee, and I.-B. Lee, *Process Identification and PID Control*. Singapore: Wiley, 2009.

[23] M. R. Patel, *Spacecraft Power Systems*. United States: CRC Press, 2005.

Mohammad Rasool Mojallizadeh received the B.Sc. degree in electrical engineering from Malekashtar University of Technology, Isfahan, Iran, in 2011 and the M.Sc. degree in control engineering from Islamic Azad University, Najafabad Branch, Isfahan, Iran, in 2013. He is currently completing his Ph.D. on control engineering at the University of Tabriz, Tabriz, Iran. His research interests include neural networks, fuzzy control theory and applied nonlinear control techniques.

Bahram Karimi received the M.Sc. degree in control engineering from Isfahan University of Technology, Isfahan, Iran, in 2000, and the Ph.D. degree in control engineering from the Amirkabir University of Technology (Poly Technique), Tehran, Iran in 2008. In 2001, he joined Malekashtar University of Technology, Isfahan, Iran, as a faculty member, and is currently an Assistant Professor of electrical engineering. His research interests include nonlinear sliding mode and adaptive control, large-scale systems, and intelligent systems.